

Continuous measurement of a charge qubit with a point contact detector at arbitrary bias: the role of inelastic tunnelling

T. M. Stace¹ and S. D. Barrett^{1,2}

¹*Cavendish Laboratory, University of Cambridge, Madingley Road, Cambridge CB3 0HE, UK**

²*Hewlett Packard Laboratories, Filton Road, Stoke Gifford Bristol, BS34 8QZ†*

(Dated: June 20, 2018)

We study the dynamics of a charge qubit, consisting of a single electron in a double well potential, coupled to a point-contact (PC) electrometer using the quantum trajectories formalism. In contrast with previous work, our analysis is valid for *arbitrary* source-drain bias across the PC, but is restricted to the sub-Zeno limit. We find that the dynamics is strongly affected by inelastic tunnelling processes in the PC. These processes reduce the efficiency of the PC as a qubit readout device, and induce relaxation even when the source-drain bias is zero. We show that the sub-Zeno dynamics are divided into two regimes: low- and high-bias in which the PC current and current power spectra show markedly different behaviour. To further illustrate the division between the regimes and the inefficiency of the detector, we present simulated quantum trajectories of the conditional qubit and detector dynamics. We also describe how single shot measurements in an arbitrary basis may be achieved in the sub-Zeno regime.

PACS numbers: 73.63.Kv 85.35.Be, 03.65.Ta, 03.67.Lx

I. INTRODUCTION

Single shot quantum measurement of mesoscopic systems is recognized as an important goal. Fundamentally, it will allow us to make time-resolved observations of quantum mechanical effects in such systems, and practically it will be a necessary component in the construction of solid-state quantum information processors (QIP). There are numerous proposals for implementing QIP in solid state systems, using doped silicon¹, electrostatically defined quantum dots² and superconducting boxes³. In these proposals, the output of the QIP is determined by measuring the position of a single electron or Cooper pair. Single electrons hopping onto single quantum dots have been observed on a microsecond time scale using single-electron transistors (SET)⁴. Ensemble measurements of a double well system (qubit) have been demonstrated in superconducting devices⁵. So far, single shot qubit measurements remain elusive.

It is therefore important to consider the measurement of single electron qubits by sensitive electrometers. Two possible electrometers have been discussed to date: SETs (see e.g. Makhlin et al.³) and point contacts (PCs)^{6–14}. PCs have been shown to be sensitive charge detectors^{15–18}, and are the focus of this work. Figure 1 illustrates the physical system we consider here, with a PC (represented by two Fermi seas separated by a tunnel barrier) in close proximity to one of the double well minima. Despite the apparent simplicity of this system it exhibits a rich range of behaviour.

There are several energy scales of relevance: the splitting of the qubit eigenstates, ϕ , the bias voltage applied across the PC, $eV = \mu_S - \mu_D$, and the measurement induced dephasing rate, Γ_d , due to the different currents through the PC that result for different localized qubit electron states. These three energies define three distinct measurement regimes

1. low-bias regime, where $\Gamma_d/2 \ll eV < \phi$.
2. high-bias regime, where $\Gamma_d/2 \ll \phi < eV$.
3. quantum Zeno limit, where $\phi \ll \Gamma_d/2 \ll eV$.

In the quantum Zeno limit, frequent weak measurements localize the qubit, suppressing its dynamics^{6,10}. To date, little attention has been paid to the low bias regime¹⁹. Recently, the *asymmetric* power spectrum was calculated for arbitrary eV ²⁰. This may correspond to the emission and absorption power spectra of quanta in the PC, as discussed in²¹. Unconditional calculations of the dynamics for arbitrary eV have also been discussed recently²².

We present a detailed analysis of the sub-Zeno limit, for arbitrary eV , showing the sharp difference in behaviour between the low- and high-bias regimes. Our analysis demonstrates the importance of inelastic tunnelling processes in the PC, in which electrons tunnelling through the PC barrier exchange energy with the qubit. These inelastic processes, illustrated in Fig. 1, incoherently excite or relax the qubit, yet are not in general experimentally distinguishable from elastic tunnelling processes using current measurement.

The paper begins with a derivation of an unconditional master equation for the joint system consisting of qubit and PC, highlighting the significance of the Fourier decomposition of the interaction Hamiltonian. We then present

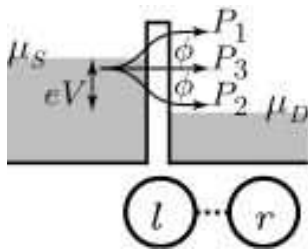


FIG. 1: Schematic of the qubit and PC showing lead energy bands. Electrons tunnelling from the source to the drain may do so elastically or inelastically, depicted by arrows. Different transitions induce different jumps, P_i , on the qubit.

analytic solutions to this master equation, in both the high- and low-bias regimes. In Sec. V, we derive *conditional* master equations, which describe the dynamics of the qubit conditioned on particular realizations of the PC detector output. In Sec. VI we apply the results of the preceding sections to determine steady state properties such as the steady state density matrix (which demonstrates the close analogy between the PC bias voltage and a heat bath), and the corresponding detector output current. Following this, we derive steady state power spectra. We end the analysis with some sample trajectories, found by solving the conditional master equations, showing possible measurement outcomes. We conclude the paper with a discussion of the implications of our results for qubit spectroscopy, and for quantum information processing.

II. SYSTEM HAMILTONIAN

We model the double well system as a two level system, on the basis that the two lowest energy eigenstates, $|e\rangle$ and $|g\rangle$ of the double well system are well separated from higher lying single particle energy eigenstates. We write these eigenstates as

$$\begin{aligned} |e\rangle &= \cos(\theta/2)|r\rangle - \sin(\theta/2)|l\rangle, \\ |g\rangle &= \sin(\theta/2)|r\rangle + \cos(\theta/2)|l\rangle, \end{aligned}$$

where $|l\rangle$ and $|r\rangle$ are the left and right localized states respectively. The Hamiltonian for the double well system, its interaction with the PC leads and the lead Hamiltonian is

$$H_{\text{sys}} = -\frac{\Delta}{2}\sigma_x - \frac{\epsilon}{2}\sigma_z = -\phi\sigma_z^{(e)}/2, \quad (1)$$

$$H_{\text{meas}} = \sum_{k,q} (T_{k,q} + \chi_{k,q}\sigma_z) a_{D,q}^\dagger a_{S,k} + \text{H.c.} \quad (2)$$

$$H_{\text{leads}} = H_S + H_D = \sum_k \omega_k (a_{S,k}^\dagger a_{S,k} + a_{D,k}^\dagger a_{D,k}) \quad (3)$$

where $\sigma_x = |l\rangle\langle r| + |r\rangle\langle l|$, $\sigma_z = |l\rangle\langle l| - |r\rangle\langle r|$, $\theta = \tan^{-1}(\frac{\Delta}{\epsilon})$, $\phi = \sqrt{\Delta^2 + \epsilon^2}$ and $\sigma_z^{(e)} = |g\rangle\langle g| - |e\rangle\langle e|$. We adopt the convention that $\chi_{k,q} < 0$ so that the left well is nearest the PC. When $\theta = 0$ the energy eigenstates coincide with the localized states, since tunnelling is effectively switched off. At $\theta = \pi/2$, the tunnelling rate, Δ , dominates the bias, ϵ , so the eigenstates are the completely delocalized states.

III. UNCONDITIONAL MASTER EQUATION

The von Neumann equation for the density matrix, R , of the bath and system is

$$\dot{R}(t) = -i[H_{\text{Tot}}, R]. \quad (4)$$

To derive the master equation for the reduced density operator, ρ , of the double well system we transform to an interaction picture with respect to the free Hamiltonian $H_0 = H_{\text{sys}} + H_{\text{leads}}$, $H_I(t) = e^{iH_0 t} H_{\text{Tot}} e^{-iH_0 t} - H_0 = e^{iH_0 t} H_{\text{meas}} e^{-iH_0 t}$, expand the von Neumann equation to second order and trace over the lead modes, i.e.

$$\dot{\rho}_I(t) = \text{Tr}_{S,D}\{-i[H_I(t), R(0)] - \int_0^t dt' [H_I(t), [H_I(t'), R(t')]]\}, \quad (5)$$

where

$$H_I(t) = \sum_{k,q} e^{-i(\omega_k - \omega_q)t} (T_{k,q} + \chi_{k,q} \sigma_z(t)) a_{D,q}^\dagger a_{S,k} + \text{H.c.} \equiv \sum_{k,q} S_{k,q}(t) a_{D,q}^\dagger a_{S,k} + \text{H.c.}, \quad (6)$$

$$\text{and } \sigma_z(t) = \begin{pmatrix} \cos(\theta) & e^{-it\phi} \sin(\theta) \\ e^{it\phi} \sin(\theta) & -\cos(\theta) \end{pmatrix} \quad (7)$$

and $S_{k,q}(t)$ is a time dependent system operator that may be written as a discrete Fourier decomposition $S_{k,q}(t) = \sum_n e^{-i(\omega_k - \omega_q + \omega_n)t} P_n$ for some time independent operators P_n and frequencies ω_n . We can write the operator $S_{k,q}(t)$ explicitly as

$$S_{k,q}(t) = e^{-it(\omega_k - \omega_q)} (e^{-it\phi} P_1 + e^{it\phi} P_2 + P_3), \quad (8)$$

where $P_1 = P_2^\dagger = \chi_{00} \sin(\theta) |g\rangle\langle e|$, $P_3 = (T_{00} + \chi_{00} \cos(\theta) \sigma_z^{(e)})$ and we have assumed that the tunnelling matrix elements $T_{k,q} = T_{00}$ and $\chi_{k,q} = \chi_{00}$ are constant over the regime of interest.

The form of $S_{k,q}(t)$ indicates that there are three possible jump processes, indicated in Fig. 1. P_3 is associated with elastic tunnelling of electrons through the PC. P_1 and P_2 are associated respectively with inelastic excitation and relaxation of electrons tunnelling through the PC accompanied by an energy transfer ϕ . This energy is provided by the qubit which relaxes or excites in response. Inelastic transitions in similar systems have been described in²¹, which calculated the current power spectrum through an *open* double well system due to shot noise through a nearby PC.

Assuming the leads are always near thermal equilibrium, $\text{Tr}_{S,D}\{a_{i,k}^\dagger R(t)\} = \text{Tr}_{S,D}\{a_{i,k} R(t)\} = 0$ and $\text{Tr}_{S,D}\{a_{i,k}^\dagger a_{n,k} R(t)\} = \delta_{i,j} f_i(\omega_k) \rho(t)$, where $i, j \in \{L, R\}$ and f_i is the Fermi distribution for lead i . We also make the common assumption²³ that if the lead correlation time is much shorter than other time scales, then the lower limit on the time integral in Eq. (5) may be set to $-\infty$. Equation (5) becomes

$$\begin{aligned} \dot{\rho}_I(t) \approx & - \int_{-\infty}^t dt' \int d\omega_k \int d\omega_q g_S(\omega_k) g_D(\omega_q) f_S(\omega_k) (1 - f_D(\omega_q)) \\ & \times (S(t)^\dagger S(t') \rho_I(t') - S(t) \rho_I(t') S(t')^\dagger - S(t') \rho_I(t') S(t)^\dagger + \rho_I(t') S(t')^\dagger S(t)) \\ & - \int_{-\infty}^t dt' \int d\omega_k \int d\omega_q g_S(\omega_k) g_D(\omega_q) f_D(\omega_q) (1 - f_S(\omega_k)) \\ & \times (S(t) S(t')^\dagger \rho_I(t') - S(t)^\dagger \rho_I(t') S(t') - S(t')^\dagger \rho_I(t') S(t) + \rho_I(t') S(t') S(t)^\dagger), \end{aligned} \quad (9)$$

where we have made the standard replacement $\sum_k \rightarrow \int d\omega_k g_{S(D)}(\omega_k)$ where $g_{S(D)}(\omega_k)$ is the density of states for lead $S(D)$ which we will hereafter assume is a constant, $g_{S(D)}$, in the energy range of interest.

We wish to evaluate the integrals in Eq. (9) at zero temperature, so to show the method and approximations used, we evaluate a particular term in Eq. (9) using the Fourier decomposition of $S(t)$:

$$\begin{aligned} & \sum_{k,q} f_S(\omega_k) (1 - f_D(\omega_q)) \int_{-\infty}^t dt' S(t) \rho_I(t') S^\dagger(t') \\ & = \sum_{mn} \int d\omega_k \int d\omega_q g_S g_D f_S(\omega_k) (1 - f_D(\omega_q)) \int_{-\infty}^t dt' e^{-i(\omega_k - \omega_q + \omega_m)t} e^{i(\omega_k - \omega_q + \omega_n)t'} P_m \rho_I(t') P_n^\dagger, \\ & \approx \pi g_S g_D \sum_{mn} \int d\omega_k \int d\omega_q f_S(\omega_k) (1 - f_D(\omega_q)) \delta(\omega_k - \omega_q + \omega_n) e^{i(\omega_n - \omega_m)t} P_m \rho_I(t) P_n^\dagger, \\ & \approx \pi g_S g_D \sum_n \int d\omega_k f_S(\omega_k) (1 - f_D(\omega_k + \omega_n)) P_n \rho_I(t) P_n^\dagger. \\ & = \pi g_S g_D \sum_n \Theta(\mu_S - \mu_D + \omega_n) P_n \rho_I(t) P_n^\dagger, \end{aligned} \quad (10)$$

where $\Theta(x) = (x + |x|)/2$ is the ramp function and μ_i is the chemical potential of lead i . The first equality follows from substituting the Fourier decomposition of $S(t)$, the second equality follows from making the Markov approximation, $\rho_I(t') \rightarrow \rho_I(t)$, the third (approximate) equality we have made a rotating-wave approximation (RWA), where we make the replacement $e^{i(\omega_n - \omega_m)t} \rightarrow \delta_{m,n}$, and finally we integrate over ω_k . The RWA is reasonable as long as $\phi \gg \nu^2 eV$, where $\nu = \sqrt{2\pi g_S g_D} \chi_{00}$ is a small quantity. This is justified when we come to integrate the master equation where

terms with $n \neq m$ are rotating sufficiently rapidly to vanish. Using the same arguments on each term in Eq. (9) results in the general form of the master equation

$$\dot{\rho}_I(t) = 2\pi g_S g_D \sum_n \left(\mathcal{D}[\sqrt{\Theta(eV + \omega_n)} P_n] \rho_I(t) + \mathcal{D}[\sqrt{\Theta(-eV - \omega_n)} P_n^\dagger] \rho_I(t) \right), \quad (11)$$

where $V = \mu_S - \mu_D$ is the bias applied across the PC, $\mathcal{D}[B]\rho = \mathcal{J}[B]\rho - \mathcal{A}[B]\rho$, $\mathcal{J}[B]\rho = B\rho B^\dagger$ and $\mathcal{A}[B]\rho = \frac{1}{2}(B^\dagger B\rho + \rho B^\dagger B)$.

We may transform the master equation, Eq. (11), back to a Schrödinger picture to reinstate the free dynamics of the double well system. It conveniently turns out that the transformation of the P_n 's back to the Schrödinger picture merely multiplies them by the unitary factor $e^{i\omega_n t}$. The Lindblad superoperators are invariant under such a transformation, so in the Schrödinger picture

$$\dot{\rho}(t) = -i[H_{\text{sys}}, \rho(t)] + \sum_n \left(H(eV + \omega_n) \mathcal{D}[c_n] \rho(t) + H(-eV - \omega_n) \mathcal{D}[c_n^\dagger] \rho(t) \right) \equiv \mathcal{L}\rho(t), \quad (12)$$

where $H(x)$ is the unit step function. For convenience, we have defined $c_n = \sqrt{\Theta(eV + \omega_n)} P_n$, so that

$$c_1 = \nu \sqrt{eV + \phi \sin(\theta)} |g\rangle \langle e|, \quad (13)$$

$$c_2 = \nu \sqrt{|eV - \phi| \sin(\theta)} |e\rangle \langle g|, \quad (14)$$

$$c_3 = \nu \sqrt{eV} \cos(\theta) \sigma_z^{(e)} + \mathcal{T} \sqrt{eV}. \quad (15)$$

We will show later, using an explicit model of the detection process, that $\mathcal{T} = \sqrt{2\pi g_S g_D} T_{00}$.

IV. ANALYTIC SOLUTIONS OF THE UNCONDITIONAL MASTER EQUATION

A. High bias regime

In the high bias regime, $H(-eV - \omega_n) = 0$ for all n , and the interaction picture master equation takes the form

$$\dot{\rho}_I(t) = \sum_n \mathcal{D}[c_n] \rho_I(t). \quad (16)$$

We can solve the unconditional master equation in this regime exactly. We present the solution in the interaction picture, since it contains the relevant decay time scales. (It is straightforward to find the corresponding dynamics in the Schrödinger picture via the transformation $\rho(t) = e^{-iH_{\text{sys}} t} \rho_I(t) e^{iH_{\text{sys}} t}$). The general solution is given by

$$\begin{aligned} \rho_{ge}(t) &= e^{-\Gamma_d(1+\cos^2(\theta))t/2} \rho_{ge}(0), \\ \rho_{gg}(t) &= \frac{\phi + eV}{2eV} - e^{-\Gamma_d \sin^2(\theta)t} \left(\frac{\phi + eV}{2eV} - \rho_{gg}(0) \right), \end{aligned} \quad (17)$$

where we have defined $\Gamma_d = 2\nu^2 eV$, consistent with⁶.

B. Low bias regime

Our analysis is also valid in the low bias regime, $\phi > eV$. The unconditional master equation in this case, in the interaction picture, may be written

$$\dot{\rho}_I(t) = \mathcal{D}[c_1] \rho_I(t) + \mathcal{D}[c_2^\dagger] \rho_I(t) + \mathcal{D}[c_3] \rho_I(t). \quad (18)$$

Again, we can solve the unconditional master equation in this regime exactly, and we give the solution in the interaction picture,

$$\begin{aligned} \rho_{ge}(t) &= e^{-(\Gamma_d \cos^2(\theta) + \nu^2 \phi \sin^2(\theta))t} \rho_{ge}(0), \\ \rho_{gg}(t) &= 1 - e^{-2\nu^2 \phi \sin^2(\theta)t} (1 - \rho_{gg}(0)). \end{aligned} \quad (19)$$

Note that at $\phi = eV$, Eqs. (17) and (19) agree.

V. CONDITIONAL MASTER EQUATIONS

It is also possible to describe the dynamics of the continuously measured charge qubit using a *conditional* master equation (CME). This describes the evolution of the state of the system, conditioned on the previous detector output. The CME is useful, since it allows individual measurement runs to be simulated, and also allows a straightforward calculation of detector output statistics, such as the average current and the power spectrum of current fluctuations. In this section, we derive a CME using an explicit model of the measurement process in terms of projective measurements of the number of electrons that have tunnelled through the PC. Our derivation follows a similar argument as that presented in²⁴ for the case of a continuously observed fluorescing atom.

Owing to the different types of allowed jump processes in each regime, we treat the high and low bias regimes separately.

A. High bias regime

In order to derive the CME in the high bias ($eV > \phi$) regime, we first consider the unconditional evolution of the qubit over a short time interval δt , which is taken to be sufficiently short that no more than one electron tunnels across the PC during this interval. This unconditional evolution can be written as a sum of two conditional terms, as

$$\rho_I(t_0 + \delta t) = \tilde{\rho}_{0c}(t_0 + \delta t) + \tilde{\rho}_{1c}(t_0 + \delta t). \quad (20)$$

Here, $\tilde{\rho}_{0c}$ is the unnormalized conditional density matrix for the qubit, corresponding to having observed zero electrons pass through the PC in the interval δt , whereas $\tilde{\rho}_{1c}$ is the unnormalized conditional density matrix for the qubit, corresponding to having observed a single electron pass through the PC, in the source to drain direction, in the same interval. In the high bias regime, tunnelling in the reverse direction (drain to source) does not conserve energy and therefore is strongly suppressed on timescales of interest, as we discuss further below. The normalization of these conditional states is chosen such that $\text{Tr} \{ \tilde{\rho}_{0(1)c}(t_0 + \delta t) \}$ is the probability that zero (one) electrons tunnelled through the PC in the interval δt .

Assuming that at time t_0 , the total density matrix for the system and detector may be written in the factorized form $\rho(t_0) \otimes |0\rangle\langle 0|$, where $|0\rangle\langle 0|$ represents the zero temperature state of the source and drain leads before any electrons have tunnelled, $\tilde{\rho}_{1c}(t_0 + \delta t)$ may be written

$$\tilde{\rho}_{1c}(t_0 + \delta t) = \text{Tr}_{S,D} \left\{ \Pi_1 U_I(t_0, t_0 + \delta t) (\rho(t_0) \otimes |0\rangle\langle 0|) U_I^\dagger(t_0, t_0 + \delta t) \Pi_1 \right\}. \quad (21)$$

Here,

$$\Pi_1 = \sum_{\alpha > k_S^F, \beta < k_D^F} a_{D,\alpha}^\dagger a_{S,\beta} |0\rangle\langle 0| a_{S,\beta}^\dagger a_{D,\alpha} \quad (22)$$

is the projector onto the subspace where only one electron has tunnelled through the PC in the source to drain direction, $U_I(t_0, t_0 + \delta t)$ is the interaction picture time evolution operator for the interval δt and $k_{S(D)}^F$ is the Fermi wavenumber for the source (drain) lead. For brevity we will suppress the range of the summation below. Note that Eq. (21) follows directly from the projection postulate of quantum mechanics.

An approximate expression for $\tilde{\rho}_{1c}(t_0 + \delta t)$ can be found by first expanding the time evolution operator up to second order in δt , i.e.

$$U_I(t_0, t_0 + \delta t) \approx 1 - i \int_{t_0}^{t_0 + \delta t} dt' H_I(t') - \int_{t_0}^{t_0 + \delta t} dt' \int_{t_0}^{t'} dt'' H_I(t') H_I(t''), \quad (23)$$

and then substituting into Eq. (21) to give

$$\tilde{\rho}_{1c}(t_0 + \delta t) = \sum_{\alpha, \beta} \langle 0 | a_{S,\beta}^\dagger a_{D,\alpha} U_I(t_0, t_0 + \delta t) | 0 \rangle \rho(t_0) \langle 0 | U_I^\dagger(t_0, t_0 + \delta t) a_{D,\alpha}^\dagger a_{S,\beta} | 0 \rangle, \quad (24)$$

$$\approx \sum_{\alpha, \beta} \int_{t_0}^{t_0 + \delta t} dt' \int_{t_0}^{t_0 + \delta t} dt'' \langle 0 | a_{S,\beta}^\dagger a_{D,\alpha} H_I(t') | 0 \rangle \rho(t_0) \langle 0 | H_I(t'') a_{D,\alpha}^\dagger a_{S,\beta} | 0 \rangle. \quad (25)$$

Note that the zeroth and second order terms in the expansion of $U_I(t_0, t_0 + \delta t)$ do not contribute to the above expression for $\tilde{\rho}_{1c}(t_0 + \delta t)$, since the expression contains a projector onto the subspace where only one electron has tunnelled through the PC.

Evaluating the integrals in Eq. (25) leads to the expression

$$\tilde{\rho}_{1c}(t_0 + \delta t) = \sum_{\alpha, \beta} [f_{\alpha\beta 1} P_1 + f_{\alpha\beta 2} P_2 + f_{\alpha\beta 3} P_3] \rho(t_0) [f_{\alpha\beta 1} P_1 + f_{\alpha\beta 2} P_2 + f_{\alpha\beta 3} P_3]^\dagger, \quad (26)$$

where P_i are the operators introduced in Sec. III, and

$$f_{\alpha\beta 1} = \delta t e^{-i(\omega_\beta - \omega_\alpha + \phi)(t_0 + \delta t/2)} \text{sinc}((\omega_\beta - \omega_\alpha + \phi)\delta t/2) H(\mu_S - \omega_\alpha) H(\omega_\beta - \mu_D), \quad (27)$$

$$f_{\alpha\beta 2} = \delta t e^{-i(\omega_\beta - \omega_\alpha - \phi)(t_0 + \delta t/2)} \text{sinc}((\omega_\beta - \omega_\alpha - \phi)\delta t/2) H(\mu_S - \omega_\alpha) H(\omega_\beta - \mu_D), \quad (28)$$

$$f_{\alpha\beta 3} = \delta t e^{-i(\omega_\beta - \omega_\alpha)(t_0 + \delta t/2)} \text{sinc}((\omega_\beta - \omega_\alpha)\delta t/2) H(\mu_S - \omega_\alpha) H(\omega_\beta - \mu_D). \quad (29)$$

For values of $\delta t \gg \phi^{-1}$, the cross terms in Eq. (26) make a very small contribution, and can be neglected. The remaining terms in Eq. (26) may be evaluated by converting the sums into integrals via the replacement $\sum_k \rightarrow \int d\omega_k g_{S(D)}(\omega_k)$ as in Sec. III. Finally, again for $\delta t \gg \phi^{-1}$, we make the following replacement in the integrands

$$\sin^2(x \delta t/2)/x^2 \rightarrow \pi \delta t \delta(x)/4. \quad (30)$$

Thus Eq. (26) reduces to

$$\tilde{\rho}_{1c}(t_0 + \delta t) = \delta t \sum_{n=1}^3 \mathcal{J}[c_n] \rho(t_0), \quad (31)$$

where the jump operators $\{c_n\}$ are given by Eqs. (13 - 15), with $\mathcal{T} = \sqrt{2\pi g_S g_D} T_{00}$.

Note that using the replacement of Eq. (30) amounts to a statement of energy conservation (on sufficiently long timescales). For this reason, processes such as reverse (drain to source) tunnelling are suppressed in the high bias regime, since they do not conserve energy.

The unnormalized state conditioned on having observed no tunnelling events in the time interval δt , $\tilde{\rho}_{0c}$, can be found by repeating the above derivation, but replacing Π_1 in Eq. (21) with $\Pi_0 = |0\rangle\langle 0|$. However, it is also possible to find $\tilde{\rho}_{0c}$ by a more direct route, by noting that the normalized, unconditional state satisfies

$$\rho_I(t_0 + \delta t) = \left(1 + \delta t \sum_{n=1}^3 \mathcal{D}[c_n] \right) \rho_I(t_0). \quad (32)$$

Combining Eqs. (20), (31) and (32), gives

$$\tilde{\rho}_{0c}(t_0 + \delta t) = \left(1 - \delta t \sum_{n=1}^3 \mathcal{A}[c_n] \right) \rho_I(t_0). \quad (33)$$

Equations (31) and (33) can be combined into a single, normalized, CME for the conditional state of the system, in the Schrödinger picture, as

$$d\rho_c(t) = dN(t) \left(\frac{\sum_{n=1}^3 \mathcal{J}[c_n]}{P_{1c}(t)} - 1 \right) \rho_c(t) + dt \left(- \sum_{n=1}^3 \mathcal{A}[c_n] \rho_c(t) + P_{1c}(t) \rho_c(t) - i[H_{\text{sys}}, \rho_c(t)] \right). \quad (34)$$

Here, $\rho_c(t)$ denotes the normalized conditional state of the system at time t , and $P_{1c}(t) = \text{Tr} \left\{ \sum_{n=1}^3 \mathcal{J}[c_n] \rho_c(t) \right\}$ is the probability density of observing a single electron tunnelling event. We have also introduced the classical stochastic increment $dN(t) \in \{0, 1\}$ which denotes the number of electron tunnelling events in the interval dt . The expectation value of this increment is given by

$$E[dN(t)] = P_{1c}(t) dt = \text{Tr} \left\{ \sum_{n=1}^3 \mathcal{J}[c_n] \rho_c(t) \right\} dt. \quad (35)$$

Note that although the CME of Eq. (34) has been written in terms of an infinitesimal time increment dt , it should be understood that in deriving the CME we have made use of a *coarse-graining* in time. In particular, neglecting the cross terms in Eq. (26) means that the derived CME neglects dynamics on fast timescales of order ϕ^{-1} . Implications of this will be discussed further in Sec. VII C.

B. Low bias regime

In the low bias ($eV < \phi$) regime, the CME must also take into account tunnelling in the reverse (drain to source) direction. Note that these reverse tunnelling events are, in principle, distinguishable from the forward tunnelling events. Thus the unconditional evolution over the interval δt may be written as the sum of *three* conditional terms:

$$\rho_I(t_0 + \delta t) = \tilde{\rho}_{0c}(t_0 + \delta t) + \tilde{\rho}_{1+c}(t_0 + \delta t) + \tilde{\rho}_{1-c}(t_0 + \delta t), \quad (36)$$

where $\tilde{\rho}_{1+c}$ ($\tilde{\rho}_{1-c}$) denotes the unnormalized conditional state of the qubit corresponding to having observed a single tunnelling event in the forward (reverse) direction in the interval δt , and $\tilde{\rho}_{0c}$ corresponds to having observed no tunnelling events in the same interval.

The derivation of the CME now proceeds in the same manner as in the high bias case, except that now three projectors are used, corresponding to the different distinguishable measurement outcomes:

$$\Pi_0 = |0\rangle\langle 0|, \quad (37)$$

$$\Pi_{1+} = \sum_{\alpha,\beta} a_{D,\alpha}^\dagger a_{S,\beta} |0\rangle\langle 0| a_{S,\beta}^\dagger a_{D,\alpha}, \quad (38)$$

$$\Pi_{1-} = \sum_{\alpha,\beta} a_{S,\alpha}^\dagger a_{D,\beta} |0\rangle\langle 0| a_{D,\beta}^\dagger a_{S,\alpha}. \quad (39)$$

The resulting CME may be written

$$d\rho_c(t) = dN^+(t) \left(\frac{\mathcal{J}[c_1] + \mathcal{J}[c_3]}{P_{1+c}(t)} - 1 \right) \rho_c(t) + dN^-(t) \left(\frac{\mathcal{J}[c_2^\dagger]}{P_{1-c}(t)} - 1 \right) \rho_c(t) \\ + dt \left(- \left\{ \mathcal{A}[c_1] + \mathcal{A}[c_2^\dagger] + \mathcal{A}[c_3] \right\} \rho_c(t) + [P_{1+c}(t) + P_{1-c}(t)] \rho_c(t) - i[H_{\text{sys}}, \rho_c(t)] \right). \quad (40)$$

Here, $dN^\pm(t) \in \{0, 1\}$ denotes the number of forward (reverse) electron tunnelling events in the interval dt . The expectation values of these increments are given by

$$E[dN^+(t)] = P_{1+c}(t)dt = \text{Tr} \{ \mathcal{J}[c_1] \rho_c(t) + \mathcal{J}[c_3] \rho_c(t) \} dt, \quad (41)$$

$$E[dN^-(t)] = P_{1-c}(t)dt = \text{Tr} \left\{ \mathcal{J}[c_2^\dagger] \rho_c(t) \right\} dt. \quad (42)$$

VI. STEADY STATE RESULTS

A. Pseudo-thermal ground state occupation

We can use the unconditional master equation in each regime to compute the unconditional, steady-state probability of the qubit to be found in its ground state. It is given by $\rho_{gg}(\infty) = \langle g | \rho(\infty) | g \rangle$. From Eqs. (17) and (19), we see that $\rho_{gg}(\infty)$ is

$$\rho_{gg}(\infty) = \begin{cases} \frac{eV + \phi}{2eV} & \text{if } \phi < eV \\ 1 & \text{if } \phi > eV \end{cases} \quad (43)$$

In contrast, the ground state occupation of a qubit in thermal equilibrium with a heat bath at temperature T is given by $\rho_{gg}^{\text{therm}}(\infty) = \frac{e^{\phi/k_B T}}{1 + e^{\phi/k_B T}}$. Figure 2 shows these two ground state probabilities for the case where $k_B T = eV/2$, and there is an evident analogy between the PC bias voltage and an external heat bath, even though the leads are each nominally at zero temperature, that is $f_{S,D}(\omega) = \text{H}(\mu_{S,D} - \omega)$. As the PC bias gets larger the relative fraction of each component of the mixture tends to $1/2$, analogously to a qubit in contact with a heat bath at very high temperature.

It has been suggested elsewhere that the PC bias acts somewhat like a heat bath¹¹, and we note that this correspondence is a natural conclusion of our analysis. It may be seen that even in the limit $eV \rightarrow 0$, the PC still causes the qubit to decay to its ground state. We can see from Eq. (19) that in this limit, the energy relaxation time is given by $\tau_r^{-1} = 2\nu^2 \phi \sin^2(\theta)$, and the dephasing time is $\tau_d^{-1} = \Gamma_d \cos^2(\theta) + \nu^2 \phi \sin^2(\theta)$. When the PC bias voltage is zero, we see that $\tau_d = 2\tau_r$, indicating that the dephasing is solely due to energy relaxation. This zero-bias dephasing arising from relaxation is the solid state analogue of the optical decay of an atom in a vacuum.

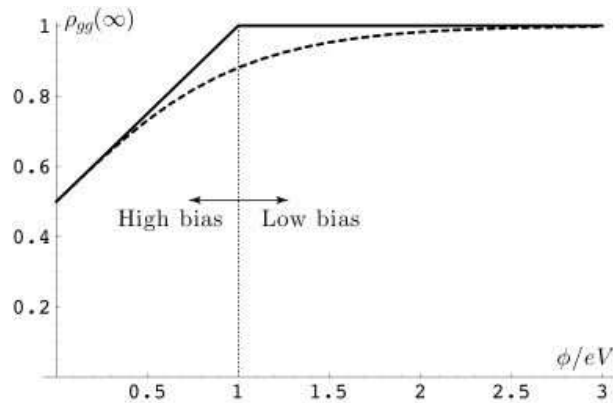


FIG. 2: Equilibrium ground state occupation probability for a qubit near a PC (solid), and the thermal equilibrium ground state occupation probability, $\rho_{gg}^{\text{therm}}(\infty)$ for a qubit in contact with a heat bath at temperature $T = eV/2$ (dashed).

This is a significant practical issue, since it means that the PC cannot be turned off merely by making the PC bias zero. To perform coherent quantum logic operations on the qubit in the presence of the PC, with error rates small enough to permit fault tolerant quantum computation, will require an extra gate to control the coupling, ν , between the qubit and the PC. ν can be significantly reduced by raising the height of the tunnel barrier between the source and drain leads of the PC. Then when the PC is off (i.e. $eV = 0$), $\nu^2\phi$ can be made much smaller than ϕ by a factor of order the fault tolerant threshold²⁵ $\sim 10^{-4}$, by raising this barrier.

B. Steady state current

The steady state current can be calculated using expectation values of the stochastic increments defined in Sec. V. In the high bias regime, the steady state current is given by $I_{ss} = eE[dN(t)/dt]_{t \rightarrow \infty} = e \text{Tr}\{\sum_{n=1}^3 \mathcal{J}[c_n]\rho(\infty)\}$. In the low bias regime, it is given by $I_{ss} = eE[(dN^+(t) - dN^-(t))/dt]_{t \rightarrow \infty} = e \text{Tr}\{\mathcal{J}[c_1]\rho(\infty) + \mathcal{J}[c_3]\rho(\infty) - \mathcal{J}[c_2^\dagger]\rho(\infty)\}$.

The current can be conveniently expressed in terms of the expected currents, I_l and I_r , for the case when the tunnelling between dots is switched off ($\theta = 0$), and the qubit is in the localized state $|l\rangle\langle l|$ or $|r\rangle\langle r|$, respectively. Then the average value of these currents is given by $\bar{I}_{\text{loc}} = \frac{I_r + I_l}{2} = e(\mathcal{T}^2 + \nu^2)eV$ and the difference is $\delta I_{\text{loc}} = I_r - I_l = -4e\nu\mathcal{T}eV$.

To first order in δI_{loc} , we find

$$I_{ss} = \begin{cases} \bar{I}_{\text{loc}} - \frac{\cos(\theta)\phi}{2eV}\delta I_{\text{loc}} = \bar{I}_{\text{loc}} - \frac{\epsilon}{2eV}\delta I_{\text{loc}} & \text{if } \phi < eV \\ \bar{I}_{\text{loc}} - \frac{\cos(\theta)\phi}{2}\delta I_{\text{loc}} = \bar{I}_{\text{loc}} - \frac{\epsilon}{2\phi}\delta I_{\text{loc}} & \text{if } \phi > eV \end{cases} . \quad (44)$$

Using I_{ss} we can compute the DC conductance

$$G = I_{ss}/V = \begin{cases} \mathcal{T}^2 + \nu^2 + 2\nu\mathcal{T}\epsilon/(eV) & \text{if } \phi < eV, \\ \mathcal{T}^2 + \nu^2 + 2\nu\mathcal{T}\epsilon/\phi & \text{if } \phi > eV, \end{cases} \quad (45)$$

in units of e^2/h . Note that these results agree with those found in Ref. 26, and given implicitly in the shot noise component of the power spectra of Ref. 19.

Equation (44) indicates that the steady state current depends on the steady state charge distribution of the qubit, which in turn depends on the qubit bias ϵ . As ϵ varies the conductance changes accordingly, which is qualitatively in agreement with observations of charge delocalization made in recent experiments^{17,18,27,28}. This behaviour is shown in Fig. 3. Note that the cusp at $\epsilon = \sqrt{(eV)^2 - \Delta^2}$ appears when $eV > \Delta$.

This result suggests an improved method for performing spectroscopy of the qubit using steady state conductance measurements through the PC: the value of the applied voltage, eV , at which a cusp in the conductance (when plotted as a function of ϵ) becomes evident *directly* gives the unbiased qubit tunnelling rate, Δ . Alternatively, observing the conductance as a function of eV , for a fixed value of ϵ , yields the splitting ϕ , by determining the voltage at which the conductance changes from low- to high-bias behaviour in Eq. (45). These methods offer a potential improvement over existing, indirect techniques²⁸, in which an estimate of Δ is extracted from a fit to a model, which in turn is limited by the uncertainty in the estimated electron temperature.

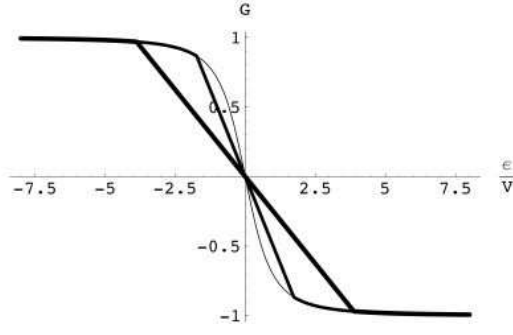


FIG. 3: The steady state conductance, G , versus e/eV , for different values of the double well tunnelling rate, (light) $eV/\Delta = 0$, (medium) $eV/\Delta = 2$ and (dark) $eV/\Delta = 4$

VII. POWER SPECTRA OF CURRENT CORRELATIONS

Using the conditional master equations, we are able to evaluate the steady state power spectrum of the two time current correlation function

$$G(\tau) = E[I(t+\tau)I(t)] - E[I(t+\tau)]E[I(t)], \quad (46)$$

and we adopt the same procedure as described in the appendix of Goan and Milburn⁶. The power spectrum is the Fourier transform of this quantity,

$$S(\omega) = 2 \int_{-\infty}^{\infty} d\tau G(\tau) e^{-i\omega\tau} = \int_0^{\infty} d\tau G(\tau) \cos(\omega\tau), \quad (47)$$

since $G(\tau) = G(-\tau)$.

A. High bias power spectrum

To compute the steady state correlation function, we take the limit $t \rightarrow \infty$, so $\rho(t) \rightarrow \rho_{\infty}$. Using the relation $I(t) dt = e dN(t)$, where $dN(t) \in \{0, 1\}$ is the number of electron tunnelling events in the time interval $(t, t+dt)$ and,

$$\begin{aligned} E[dN(t+\tau)dN(t)] &= \text{Prob}[dN(t) = 1]E[dN_c(t+\tau)|_{dN(t)=1}], \\ \text{Prob}[dN(t) = 1] &= dt \text{Tr} \{ \tilde{\rho}_{1c}(t+dt) \}, \\ E[dN_c(t+\tau)|_{dN(t)=1}] &= dt \text{Tr} \left\{ \sum_n \mathcal{J}[c_n] E[\tilde{\rho}_{1c}(t+\tau)|_{dN(t)=1}] \right\}, \\ E[\tilde{\rho}_{1c}(t+\tau)|_{dN(t)=1}] &= e^{\mathcal{L}\tau} \tilde{\rho}_{1c}(t+dt) / \text{Tr} \{ \tilde{\rho}_{1c}(t+dt) \}, \\ dN(t)^2 &= dN(t), \end{aligned} \quad (48)$$

we obtain the correlation function in the high bias regime for $\tau > dt$

$$G_{\text{hb}}(\tau) = \begin{cases} e^2 (\text{Tr} \{ \sum_{n,n'} \mathcal{J}[c_n] e^{\mathcal{L}\tau} \mathcal{J}[c_{n'}] \rho_{\infty} \} - \text{Tr} \{ \sum_n \mathcal{J}[c_n] \rho_{\infty} \}^2) & \text{for } \tau > dt, \\ e^2 \text{Tr} \{ \sum_n \mathcal{J}[c_n] \rho_{\infty} \} \delta(\tau) & \text{for } \tau = dt. \end{cases} \quad (49)$$

We write $G_{\text{hb}}(\tau)$ in terms of \bar{I}_{loc} and δI_{loc} :

$$G_{\text{hb}}(\tau) = e(\bar{I}_{\text{loc}} - \delta I_{\text{loc}} \frac{\phi}{2eV} \cos(\theta)) \delta(\tau) + e^{-\Gamma_d \sin^2(\theta)\tau} e^2 \left(1 - \frac{\phi^2}{(eV)^2} \right) \nu^2 (2\mathcal{T}eV \cos(\theta) + \nu\phi \sin^2(\theta))^2. \quad (50)$$

Dropping the small term $\nu\phi \sin^2(\theta)$, which is formally equivalent to keeping only the lowest order term in a series expansion in δI_{loc} , and taking the Fourier transform gives

$$S_{\text{hb}}(\omega) = S_0 - e\delta I_{\text{loc}} \frac{\phi}{V} \cos(\theta) + \frac{\delta I_{\text{loc}}^2 \Gamma_d \left(1 - \frac{\phi^2}{(eV)^2} \right) \sin^2(2\theta)}{4(\Gamma_d^2 \sin^4(\theta) + \omega^2)} \quad (51)$$

where $S_0 = 2e\bar{I}_{\text{loc}}$.

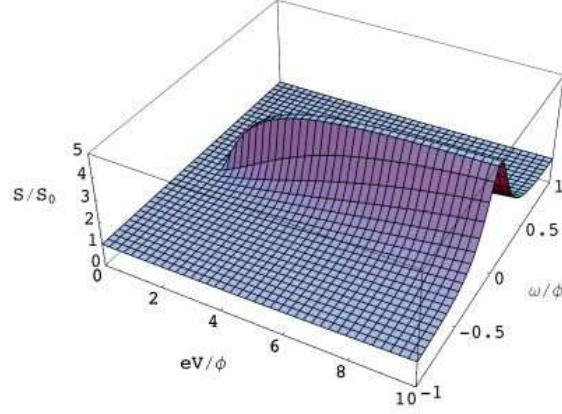


FIG. 4: Power spectra, $S(\omega)/S_0$, computed in this paper using Eqs. (51) and (54), as a function of eV/ϕ for $\theta = \pi/4$, $\nu^2 = 0.02$.

B. Low bias power spectrum

The correlation function in the low bias regime turns out to be time independent. In this regime, there are two distinguishable jump processes that can occur: source to drain electron tunnelling (both elastic and inelastic), and drain to source tunnelling (inelastic only). Therefore the current is related to the number of jumps in the time interval by $I(t) dt = e(dN^+(t) - dN^-(t))$, where $dN^{+(-)}(t)$ counts the number of source-to-drain (drain-to-source) tunnelling events in the time interval $(t, t + dt)$.

To evaluate the expectation values in $G(\tau)$, we use slightly generalized versions of Eqs. (48), for instance

$$\begin{aligned} \text{Prob}[dN^\pm(t) = 1] &= dt \text{Tr} \{ \tilde{\rho}_{1\pm c}(t + dt) \}, \\ E[dN_c^x(t + \tau) |_{dN^y(t)=1}] &= dt \text{Tr} \{ \mathcal{J}^x E[\tilde{\rho}_1 c(t + \tau) |_{dN^y(t)=1}] \} \text{ for } x, y = \pm. \end{aligned}$$

As before, to compute the steady state power spectrum, we make the replacement $\rho(t) \rightarrow \rho_\infty = |g\rangle\langle g|$, for the low bias regime. It is evident that $\mathcal{J}^- \rho_\infty = \mathcal{J}[c_2^\dagger] \rho_\infty = \mathcal{J}[c_1] \rho_\infty = 0$, so we find that

$$\begin{aligned} G_{\text{lb}}(\tau) &= \begin{cases} e^2 (\text{Tr} \{ \mathcal{J}[c_3] e^{\mathcal{L}\tau} \mathcal{J}[c_3] \rho_\infty \} - \text{Tr} \{ \mathcal{J}[c_3] \rho_\infty \}^2) & \text{for } \tau > dt, \\ e^2 \text{Tr} \{ \mathcal{J}[c_3] \rho_\infty \} \delta(\tau) & \text{for } \tau = dt. \end{cases} \quad (52) \\ &= e^2 (\mathcal{T} + \nu \cos(\theta))^2 eV \delta(\tau) \quad (53) \end{aligned}$$

Thus, the steady state low bias current correlation function is just due to elastic tunnelling through the PC. The low bias power spectrum is

$$S_{\text{lb}}(\omega) = S_0 - e \delta I_{\text{loc}} \cos(\theta) + O(\delta I_{\text{loc}}^2). \quad (54)$$

The power spectra computed in this paper are shown in Fig. 4 for $\nu^2 = 0.02$. Note the sharp change at $eV = \phi$.

C. Comparison with previous results

The work presented here is valid when $\Gamma_d \ll \phi$, whilst previous work has dealt with the large bias limit, $\phi \ll eV$ ^{6,9,10}. These limits are shown schematically in Fig. 5(a). The limit $\Gamma_d \ll \phi \ll eV$ is common to both this work and previous analyses^{6,9,10}, so we can compare the predictions of each in this limit.

The current correlation function, $G_{\text{GM}}(\tau)$, given in⁶ (subscript GM denotes the authors initials) is only valid for $\epsilon = 0$, but it is straightforward to calculate the general result, which is useful in order to compare our results with previous work. We present the general calculation in Appendix A. Figure 5(b) shows the power spectra computed in this paper (dark) and using $G_{\text{GM}}(\tau)$ (light) for large bias, $\phi/eV = 0.01$, and weak coupling, $\Gamma_d = 0.1$. The central peak at $\omega = 0$, due to inelastic transitions between the qubit energy eigenstates, shows good agreement between the results. There is a marked difference between the spectra at frequencies near $\pm\phi$. In particular the peaks predicted in⁶ are absent from our results. However, this difference can be understood by noting that, in deriving our CME in Sec. V, we have employed a temporal ‘coarse graining’, which implies that our CME does not describe dynamics on

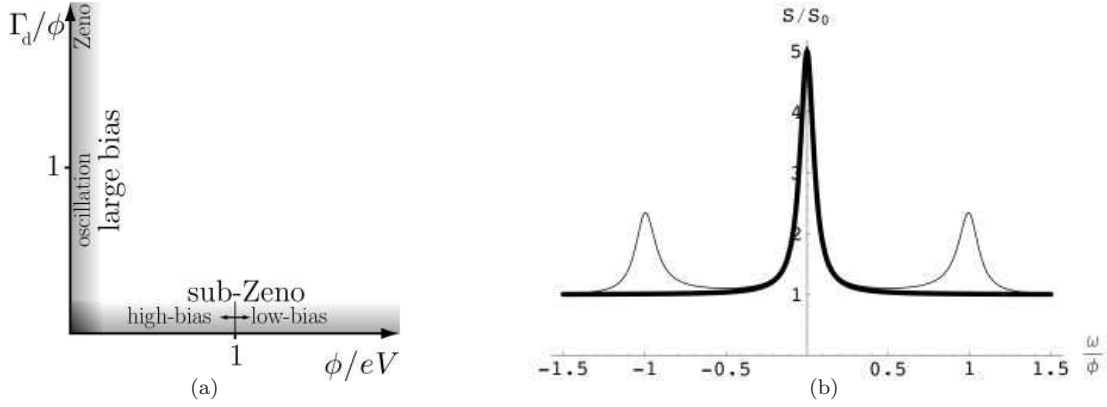


FIG. 5: (a) Phenomena predicted in this paper (sub-Zeno) and previous work (large bias). (b) The power spectrum computed in this paper with $\Gamma_d = 0.1$, $\theta = \pi/4$ and $eV = 100\phi$ (dark), and the power spectrum computed by⁶, (see appendix A), with the same parameters (light).

short timescales of order ϕ^{-1} . Therefore, our expressions for the power spectra (which are derived from our CME) are valid only for frequencies $\omega \ll \phi$.

In the low bias case, we predict a completely flat power spectrum (Eq. (54)). Although this prediction is also based on a coarse-grained CME, there is reason to expect that this should be valid at all frequencies. In particular, since the qubit rapidly relaxes to the (pure) ground state $|g\rangle$, which is a stationary state, there should be no oscillatory signal in the PC current, and no peaks in $S_{\text{Ib}}(\omega)$ should be seen at $\omega = \phi$. This prediction is in agreement with those made independently in Ref.²⁰.

VIII. MEASUREMENT TIME

The detector partially projects the qubit onto the energy eigenbasis, as seen in the form of jump operator c_3 . The energy eigenbasis is therefore the ‘preferred’ basis for the detector.

An important quantity of interest is the measurement time. This is the time taken for the measurement to project a qubit initially prepared in an equal superposition of energy eigenstates onto one or other of them. We therefore take $\rho(0) = (|e\rangle + |g\rangle)(\langle e| + \langle g|)/2$. Following Goan et al.⁷, we compute the rate of change of $E[dz_c^2(0)] \equiv E[\text{Tr}\{\sigma_z^{(e)} d\rho_c(0)\}^2]$.

We present the calculation for high bias, and note that we obtain the same result for low bias. Using the fact that

$$d\rho_c(t) = \rho_c(t + dt) - \rho_c(t) = dN(t)\rho_{1c}(t + dt) + (1 - dN(t))\rho_{0c}(t + dt) - \rho_c(t), \quad (55)$$

$dN(t)^2 = dN(t)$ and $\text{Tr}\{\sigma_z^{(e)} \rho(0)\} = 0$, we find that to first order in dt

$$\begin{aligned} E[dz_c^2(0)] &= E[dN(0) \text{Tr}\{\sigma_z^{(e)} \rho_{1c}(dt)\}^2]/2, \\ &= \frac{\text{Tr}\{\sigma_z^{(e)} \tilde{\rho}_{1c}(dt)\}^2}{2 \text{Tr}\{\tilde{\rho}_{1c}(dt)\}}, \\ &= \Gamma_d \cos^2(\theta) dt + O(\nu^3 \phi). \end{aligned} \quad (56)$$

Thus the measurement time is $\tau_m^{-1} = \Gamma_d \cos^2(\theta) + O(\nu^3 \phi)$. We note that $\tau_m \geq \tau_d$, where τ_d is the dephasing time for decay of the off diagonal elements in Eqs. (17) and (19), with equality only when $\theta = 0$. This indicates that the detector is inefficient unless the qubit energy eigenstates are localized.

IX. QUANTUM TRAJECTORIES

In Figs. 6(a) and 6(b) we show two different quantum trajectory simulations for $\theta = 0$, using the same parameters to generate both (see caption for values). We show the conditional probability (dark, solid line), $\langle l|\rho_c(t)|l\rangle$, and unconditional probability (dark, dashed line), $\langle l|\rho(t)|l\rangle$, of the qubit to be in the left well. Also shown is the purity of conditional state (light, solid), $\text{Tr}\{\rho_c(t)^2\}$, and of the unconditional state $\text{Tr}\{\rho(t)^2\}$, (light, dashed). We also show a histogram of the number of jump processes that were encountered in each time window, and this corresponds to

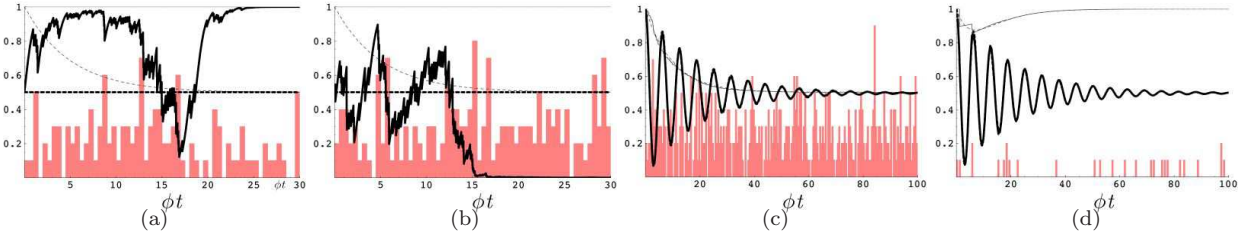


FIG. 6: (a) & (b) Showing distinct simulations where the qubit collapses to $|l\rangle$ and $|r\rangle$ respectively [for $\theta = 0, eV/\phi = 10, \nu^2 = 0.005, \mathcal{T}^2 = 0.5$]. At $\theta = \pi/2$ currents are uncorrelated with the qubit in either (c) high-bias [$eV/\phi = 10, \nu^2 = 0.005, \mathcal{T}^2 = 0.5$] or (d) low-bias [$eV/\phi = 0.5, \nu^2 = 0.05, \mathcal{T}^2 = 0.5$]. In all panels, dark curves are $\langle l|\rho_c(t)|l\rangle$ (solid) and $\langle l|\rho(t)|l\rangle$ (dashed), and light curves are the conditional purity $\text{Tr}\{\rho_c(t)^2\}$ (solid) and unconditional purity $\text{Tr}\{\rho(t)^2\}$ (dashed). Histograms show the number of jumps per time interval, (scaled by $1/10$).

experimentally measured currents. In all trajectories shown in this paper, the histograms are scaled by the factor $\frac{1}{10}$, and are mutually comparable. In these two figures, the initial state of the system is chosen to be the pure state $(|l\rangle + |r\rangle)/\sqrt{2}$.

The evolution of the measurement clearly shows the qubit collapsing to the state $|l\rangle$ or $|r\rangle$, and the state remains pure throughout. This is because, at $\theta = \pi/2$, the inelastic jump operators c_1 and c_2 are suppressed, and the remaining jump operator c_3 partially projects the state onto the localized basis. The average current, determined by the mean of the histogram is higher in the case where the qubit collapsed onto the state $|r\rangle$, which is consistent with physical intuition, since in this configuration, the tunnelling rate through the PC is highest. The fact that the unconditional probability to find the electron on the left well is constant at 0.5 reflects the fact that the state of the system collapses to $|l\rangle$ or $|r\rangle$ with equal probability, consistent with the initial state preparation being an equal superposition of the localized states, and thus for $\theta = 0$, the PC serves as a good quantum non-destructive (QND) measurement device.

Figures 6(d) and 6(c) shows the dynamics of the system for $\theta = \pi/2$ in the high bias ($eV/\phi = 2$) and low bias ($eV/\phi = 0.5$) regimes, respectively. In both cases, the initial state of the system is $|l\rangle$.

As predicted by Eq. (17), in the high bias limit the equilibrium state of the system is an unequal mixture of $|g\rangle$ and $|e\rangle$. We may calculate the unconditional steady state purity, and we find $\text{Tr}\{\rho(\infty)\} = \frac{(eV)^2 + \phi^2}{(2eV)^2} = 0.505$ for the parameters used. This agrees with the simulation of Fig. 6(d), where the conditional and unconditional evolution is very similar.

Similar comments apply to Fig. 6(c), however the unconditional steady state is always $|g\rangle$ for the low bias limit, which is of course a pure state, and for the case considered is just an equal superposition of localized states $|g\rangle = (|l\rangle + |r\rangle)/\sqrt{2}$. Thus the probability for the qubit to be in the left well is just the same as for Fig. 6(d), but the equilibrium state is pure.

We illustrate the effect of changing parameters in Fig. 7. We show simulated trajectories for five different bias voltages, $eV = 0.5, 1, 2$ and 4 , and for three different mixing angles $\theta = \pi/8, \pi/4$ and $3\pi/8$. In the high bias regime, and small values of θ there are fluctuations that bear a superficial resemblance to the quantum Zeno effect (QZE). The state of the qubit tends to fluctuate between mixtures of energy eigenstates, and the conditional density matrix is diagonal in the energy eigenbasis, with off-diagonal terms being negligible in this basis.

This resemblance to the QZE is only superficial however. In the QZE, the free dynamics of the qubit are suppressed due to the strong and frequent measurement which project the system into pure, localized states $\{|l\rangle, |r\rangle\}$. The sharp transitions that occur in the QZE result from the small probability for the electron to make a transition between sites which is realized as a rapid, occasional tunnelling event.

In contrast, the transitions that are evident in Fig. 7 for small θ are due to relaxation or excitation of the qubit, accompanied by inelastic tunnelling processes through the PC, rather than the ‘collapse of the wavefunction’ due to accumulated information about the qubit in the case of the QZE. As θ increases, the transitions become smaller in amplitude and less distinct, until $\theta = \pi/2$ when inelastic tunnelling events through the PC dominate the current and the qubit state is damped to the completely mixed state.

At the transition from low bias to high bias, $eV/\phi = 1$, fluctuations begin to appear in the steady state trajectory. For $eV < \phi$ the conditional steady state of the qubit is constant, whereas for $eV > \phi$ the conditional steady state shows fluctuations which increase with increasing bias voltage.

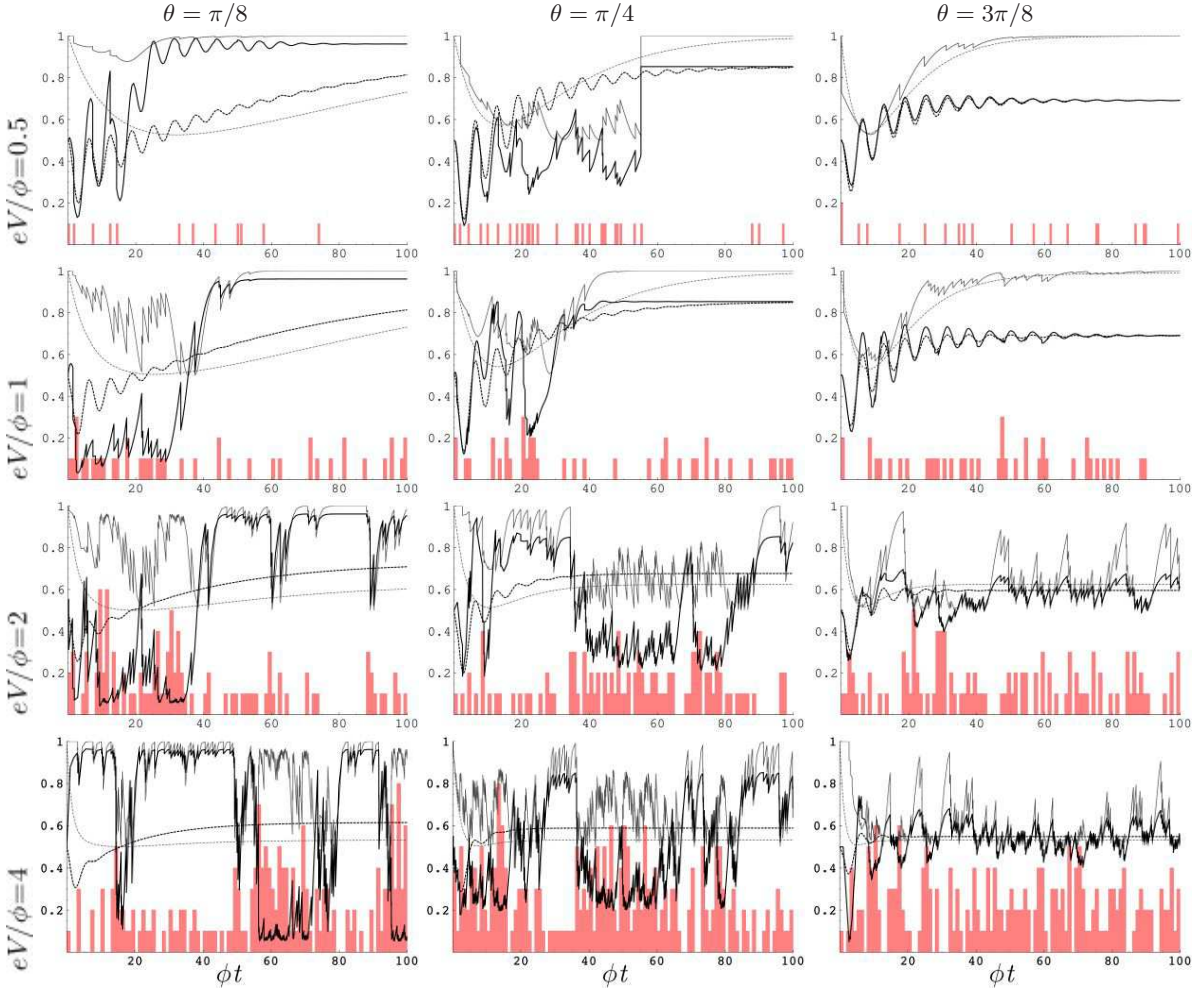


FIG. 7: Simulated trajectories from left to right, $\theta = \pi/8, \pi/4$ and $3\pi/8$. From top to bottom, $eV/\phi = 0.5, 0.9, 1.1, 2$ and 4 . In all $\nu^2 = 0.05$ and $\mathcal{T}^2 = 0.5$. In each panel, the dark curves are $\langle l|\rho_c(t)|l \rangle$ (solid) and $\langle l|\rho(t)|l \rangle$ (dashed), and the light curves are the purity of the conditional state $\text{Tr}\{\rho_c(t)^2\}$ (solid) and the unconditional state $\text{Tr}\{\rho(t)^2\}$ (dashed). The histogram shows the number of jumps that occurred in each time interval. The histograms are all scaled by the same factor, so are comparable with one another. Reverse tunnelling events are responsible for the sharp changes in the first two panels.

X. DISCUSSION

The predictions of this work should be experimentally verifiable. In particular, it should be possible, in near-future experiments, to observe the qualitative change in both the steady state current, and the fluctuations in the current, in the transition from the low- to high-bias regimes. This sharp transition between low- and high-bias regimes also provides possible techniques for performing spectroscopy of solid state qubits, as discussed in Sec. VI B.

The results presented here describe the dynamics of the measured qubit in the sub-Zeno limit, $\Gamma_d \ll \phi$, for arbitrary PC bias eV , whereas previous analyses^{6,9,10,13} are valid only for large PC bias, $eV \gg \phi$, but arbitrary Γ_d/ϕ . Outside these regimes, for finite ratios Γ_d/ϕ and eV/ϕ neither approach is formally valid, and non-Markovian effects may play a significant role. This parameter regime is therefore an open area for investigation.

There are a number of practical issues that the present paper raises. Firstly, as discussed earlier, to turn the measurement off, it is not enough just to turn the PC bias to zero. Simultaneously one must also make ν^2 small, which can be accomplished with extra surface gates.

Secondly, in order to perform a good single-shot measurement we require that the qubit measurement time is much shorter than the detector-induced relaxation time,³ i.e. $\tau_m \ll \tau_r$. From Eqs. (17), (19) and (56) we see that $\tau_r^{-1} = 2\nu^2 \max(\phi, eV) \sin^2(\theta)$ and $\tau_m^{-1} = 2\Gamma_d \cos^2(\theta)$, so we require that $\sin(\theta) \approx 0$. Therefore, our work indicates that measurements in the sub-Zeno regime are not possible for highly delocalized qubit eigenstates. Furthermore, ideal measurements (i.e. measurements for which the conditional state remains pure) are only attainable when $\theta = 0$,

so the energy eigenstates are the localized states.

In order to perform good single-shot measurements, one could operate in the Zeno regime, though there may be technical difficulties in obtaining a sufficiently large value of Γ_d , since this requires passing large currents through the PC. These large currents can, in turn, lead to heating in the detector, which can significantly increase noise and lead to additional decoherence of the qubit.^{17,29}

Alternatively, performing a good single-shot measurement in the sub-Zeno regime consists of three tasks:

1. Localise the qubit eigenstates by turning on the qubit bias (ϵ) and/or decreasing qubit tunnelling rate (Δ), so $\theta \approx 0$.
2. Increase the lead tunnelling rate (T_{00} and χ_{00}) by lowering a tunnel barrier.
3. Turn on the lead bias voltage (V).

The rate at which θ is varied effects a rotation on the qubit, so by selecting this rate appropriately, we can choose to measure in an arbitrary basis.

XI. CONCLUSION

In this paper we have used the quantum trajectories formalism to derive master equations for measurements of a charge qubit by an external point contact electrometer in the sub-Zeno regime. The master equation was derived without recourse to heuristic arguments, and resulted in the inclusion of inelastic processes in which energy is exchanged between the qubit and the detector. These inelastic processes have a profound effect on the conditional and unconditional dynamics of the system. Furthermore, within the sub-Zeno regime, our results are valid for arbitrary detector bias voltage.

In the low-bias regime ($eV < \phi$) the qubit always relaxes to its ground state, much like a qubit in equilibrium with a zero-temperature bath. In this case, relaxation to the ground state is due to the eventual spontaneous relaxation of the qubit accompanied by an excitation of a PC lead electron. The corresponding steady state power spectrum is flat.

In the high-bias regime ($eV > \phi$) the PC leads act like a zero-entropy heat bath at non-zero temperature and both inelastic relaxation and excitation processes take place, causing the steady state of the qubit to be a mixture of excited and ground states. These inelastic transitions are also reflected in the power spectrum, which exhibits a peak centered at zero frequency, corresponding to transitions of the qubit between the localized energy eigenstates.

The sharp transition the dynamics at $eV = \phi$ is also reflected in the steady state conductance of the PC. This observation provides techniques for accurately determining the qubit Hamiltonian parameters directly from conductance measurements.

Single shot measurement remains possible in the sub-Zeno regime, provided that the system Hamiltonian is modified such that the energy eigenstates become localized before the measurement takes place. This also gives the added freedom that we may choose an arbitrary basis in which to measure.

TMS thanks the Hackett committee, the CVCP and Fujitsu for financial support. SDB acknowledges support from the E.U. NANOMAGIQC project (Contract no. IST-2001-33186). We thank H.-S. Goan, W. J. Munro, T. Spiller, G. J. Milburn, H.-A. Engel, R. Aguado, A. Shnirman, H. M. Wiseman and D. Averin for useful conversations. In particular, H. M. Wiseman suggested Fig. 5(a).

APPENDIX A: GENERALIZED POWER SPECTRUM OF GOAN AND MILBURN⁶

The power spectra calculated in⁶ assumed $\epsilon = 0$. In order to compare our power spectra with theirs for arbitrary parameter values, we derive the power spectra for their model for arbitrary ϵ .

It is laborious to compute $G_{\text{GM}}(\tau)$ directly, however since we are only interested in the power spectrum, we can bypass the explicit solution for the correlation function in the time domain and calculate the power spectrum directly.

We wish to compute the Fourier transform, F , of equation (A8) of⁶ (hereafter called (GMA8)). This may be done via a Laplace transform, L , using the relation for a symmetric function $f(t)$

$$F_{\omega}[f(t)] = L_{i\omega}[f(t)] + L_{-i\omega}[f(t)]. \quad (\text{A1})$$

The Laplace transform of (GMA8) is

$$L_s[G_{\text{GM}}(\tau)] = e \bar{I}_{\text{loc}} + \delta I_{\text{loc}}^2 (\text{Tr}\{n_1 L_s[e^{\mathcal{L}\tau} n_1 \rho_{\infty}]\} - \text{Tr}\{n_1 \rho_{\infty}\}^2 / s). \quad (\text{A2})$$

The notation $e^{\mathcal{L}\tau}n_1\rho_\infty$ is just shorthand for the solution to the unconditional master equation (GM5a) at time τ subject to the initial condition $\rho(0) = n_1\rho_\infty = n_1/2$. Taking the Laplace transform of (GM5a) gives

$$s\mathbf{L}_s[\rho(t)] - \rho(0) = -i[H_{\text{sys}}, \mathbf{L}_s[\rho(t)]] + \mathcal{D}[T_l + (T_r - T_l)n_1]\mathbf{L}_s[\rho(t)]. \quad (\text{A3})$$

$\mathbf{L}_s[\rho(t)]$ may be found straightforwardly from this expression and then $\mathbf{L}_s[e^{\mathcal{L}\tau}n_1\rho_\infty]$ is obtained by substituting $\rho(0) \rightarrow n_1\rho_\infty = n_1/2$ into $\mathbf{L}_s[\rho(\tau)]$, though it is a somewhat cumbersome expression. Evaluating the traces in Eq. (A2) yields

$$\mathbf{L}_s[G_{\text{GM}}(\tau)] = \frac{e\bar{I}_{\text{loc}}}{2} + \delta I_{\text{loc}}^2 \frac{4s^2 + 2\phi^2 + 4s\mathcal{X}^2 + \mathcal{X}^4 + 2\phi^2 \cos(2\theta)}{4(4s^3 + 4s^2\mathcal{X}^2 + \phi^2\mathcal{X}^2 + s(4\phi^2 + \mathcal{X}^4) - \phi^2\mathcal{X}^2 \cos(2\theta))}, \quad (\text{A4})$$

where we have used the same definition of \mathcal{X} as found in Goan and Milburn⁶, which for comparison is given in our notation as $\mathcal{X} = \nu\sqrt{e\bar{V}}$. The power spectrum is then given by

$$S_{\text{GM}}(\omega) = 2\mathbf{F}_\omega[G_{\text{GM}}(t)] = 2(\mathbf{L}_{i\omega}[G_{\text{GM}}(\tau)] + \mathbf{L}_{-i\omega}[G_{\text{GM}}(\tau)]) \quad (\text{A5})$$

* Electronic address:

† Electronic address:

- ¹ B. E. Kane, *Nature* **393**, 133 (1998).
- ² D. Loss and D. P. DiVincenzo, *Phys. Rev. A* **57**, 120 (1998).
- ³ Y. Makhlin, G. Schon, and A. Shnirman, *Rev. Mod. Phys.* **73**, 357 (2001).
- ⁴ W. Lu, Z. Ji, L. Pfeiffer, K. W. West, and A. J. Rimberg, *Nature* **423**, 422 (2003).
- ⁵ Y. A. Pashkin, T. Yamamoto, O. Astafiev, Y. Nakamura, D. V. Averin, and J. S. Tsai, *Nature* **421**, 823 (2003).
- ⁶ H.-S. Goan and G. J. Milburn, *Phys. Rev. B* **64**, 235307 (2001).
- ⁷ H.-S. Goan, G. J. Milburn, H. M. Wiseman, and H. B. Sun, *Phys. Rev. B* **63**, 125326 (2001).
- ⁸ S. A. Gurvitz, *Phys. Rev. B* **56**, 15215 (1997).
- ⁹ A. N. Korotkov, *Phys. Rev. B* **63**, 085312 (2001).
- ¹⁰ A. N. Korotkov and D. V. Averin, *Phys. Rev. B* **64**, 165310 (2001).
- ¹¹ D. Mozyrsky and I. Martin, *Phys. Rev. Lett.* **89**, 018301 (2002).
- ¹² S. Pilgram and M. Büttiker, *Phys. Rev. Lett.* **89**, 200401 (2002).
- ¹³ S. A. Gurvitz, L. Fedichkin, D. Mozyrsky, and G. P. Berman, arxiv:cond-mat/0301409 (2003).
- ¹⁴ Y. Makhlin, G. Schon, and A. Shnirman, *Phys. Rev. Lett.* **85**, 4578 (2000).
- ¹⁵ M. Field, C. G. Smith, M. Pepper, D. A. Ritchie, J. E. F. Frost, G. A. C. Jones, and D. G. Hasko, *Phys. Rev. Lett.* **70**, 1311 (1993).
- ¹⁶ E. Buks, R. Schuster, M. Heiblum, D. Mahalu, and V. Umansky, *Nature* **391**, 871 (1998).
- ¹⁷ S. Gardelis, C. G. Smith, J. Cooper, D. A. Ritchie, E. H. Linfield, Y. Jin, and M. Pepper, *Phys. Rev. B* **67**, 073302 (2003).
- ¹⁸ J. M. Elzerman, R. Hanson, J. S. Greidanus, L. H. Willems van Beveren, S. DeFranceschi, L. M. K. Vandersypen, S. Tarucha, and L. P. Kouwenhoven, *Phys. Rev. B* **67**, 161308 (2003).
- ¹⁹ T. M. Stace and S. D. Barrett, *Phys. Rev. Lett.* **92**, 136802 (2004), .
- ²⁰ A. Shnirman, D. Mozyrsky, and I. Martin, arXiv:cond-mat/0211618 (2002).
- ²¹ R. Aguado and L. P. Kouwenhoven, *Phys. Rev. Lett.* **84**, 1986 (2000).
- ²² X.-Q. Li, W.-K. Zhang, P. Cui, J. Shao, Z. Ma, and Y. Yan, *Physical Review B* **69**, 085315 (pages 9) (2004), .
- ²³ C. W. Gardiner and P. Zoller, *Quantum Noise* (Springer, 2000).
- ²⁴ H. P. Breuer and F. Petruccione, *The theory of Open Quantum Systems* (Oxford University Press, Oxford, 2002).
- ²⁵ J. Preskill, *Proc. Roy. Soc. Lond.* **A454**, 385 (1998).
- ²⁶ H.-A. Engel, V. Golovach, D. Loss, L. M. K. Vandersypen, J. M. Elzerman, R. Hanson, and L. P. Kouwenhoven, cond-mat/0309023 (2003).
- ²⁷ A. W. Rushforth, C. G. Smith, M. D. Godfrey, H. E. Beere, D. A. Ritchie, and M. Pepper, *Physical Review B (Condensed Matter and Materials Physics)* **69**, 113309 (pages 4) (2004), .
- ²⁸ L. DiCarlo, H. J. Lynch, A. C. Johnson, L. I. Childress, K. Crockett, C. M. Marcus, M. P. Hanson, and A. C. Gossard, *Physical Review Letters* **92**, 226801 (2004), .
- ²⁹ S. D. Barrett, Ph.D. thesis, University of Cambridge (2003).